01 Jan 2003

Analysis of Simple Two-Capacitor Low-pass Filters

Todd H. Hubing
Missouri University of Science and Technology

David Pommerenke
Missouri University of Science and Technology, davidjp@mst.edu

Theodore M. Zeeff

Thomas Van Doren
Missouri University of Science and Technology

Recommended Citation

T. H. Hubing et al., "Analysis of Simple Two-Capacitor Low-pass Filters," *IEEE Transactions on Electromagnetic Compatibility*, Institute of Electrical and Electronics Engineers (IEEE), Jan 2003.
The definitive version is available at https://doi.org/10.1109/TEMC.2003.819059

Analysis of Simple Two-Capacitor Low-Pass Filters

Theodore M. Zeeff, Todd H. Hubing, *Senior Member, IEEE*, Thomas P. Van Doren, *Fellow, IEEE*, and David Pommerenke, *Member, IEEE*

***Abstract*—The performance of typical low-pass capacitor filters is limited by the mutual inductance between the input and output sides of the filter. This paper describes how two appropriately spaced capacitors can be used to construct a low-pass filter with significantly better high-frequency performance than a one-capacitor filter. Laboratory measurements and numerical simulations are used to quantify the mutual inductance and compare the performance of one- and two-capacitor low-pass filters.**

***Index Terms*—I/O filtering, low-pass filters, mutual inductance.**

I. Introduction

LOW-SPEED I/O traces on a printed circuit board (PCB) must often be filtered to keep high-frequency noise from exiting the PCB on an attached cable. A typical low-cost, low-pass filter is a single capacitor connected between the signal trace and the return plane of the PCB. This type of filter can be effective up to a few hundred megahertz. However, the current flowing through the capacitor couples magnetic flux from one side of the filter to the other. At higher frequencies, the impact of this mutual inductance has been shown to be the dominant factor limiting the effectiveness of capacitor filters [1], [2]. This paper shows that two capacitors with appropriate spacing can be used to build inexpensive low-pass filters that are much more effective than single-capacitor filters.

II. Background Information on Low-Pass Filters

A schematic of a typical low-pass filter capacitor including the parasitic inductances associated with the layout is shown in Fig. 1. The schematic has a source voltage V_s with a source resistance R_s driving load resistance R_L with a shunt capacitor acting as a low-pass filter. The capacitor has an equivalent series resistance *R* and a capacitance *C*. The source-side loop and the load-side loop have a self-inductance of L_1 and L_2, respectively. Additionally, there is a mutual inductance *M* between both halves of the circuit. The mutual inductance results from the magnetic flux that wraps the body of the capacitor and its connections to the board. This flux couples the input loop to the output loop.

The impact of the mutual inductance on the voltage transfer coefficient at high frequencies, and therefore on the effectiveness of the capacitor as a low-pass filter, is shown in Fig. 2 as a bode plot of $|S_{21}|$ for the case where $R_s = R_L = Z_o$ Above the resonance frequency $1/(MC)^{1/2}$, $|S_{21}|$ is proportional to *M*. Above the frequency $Z_0/(L+M)$, $|S_{21}|$ is equal to *M/L* or k_{12} (where $k_{xy} = (M_{xy})/(\sqrt{L_x L_y})$).

If the mutual inductance between the source-side loop and the load-side loop is reduced, then the voltage transfer characteristics will improve (low $|S_{21}|$) at high frequencies.

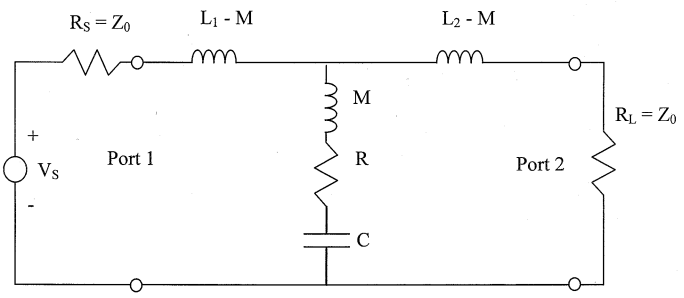

Fig. 1. Equivalent circuit of a low-pass filter.

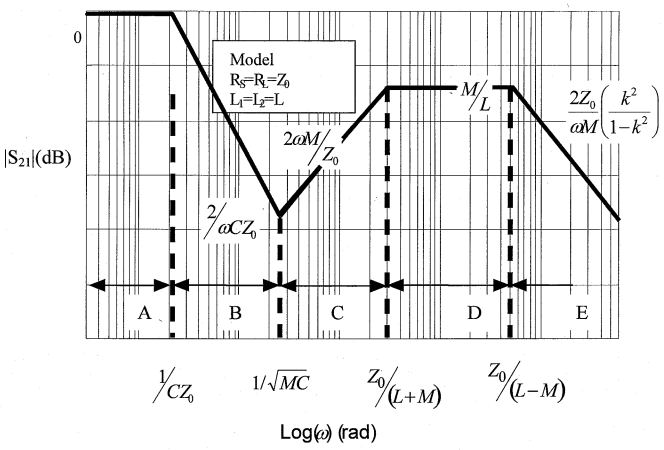

Fig. 2. Bode plot of $|S_{21}|$ of the low-pass filter in Fig. 1.

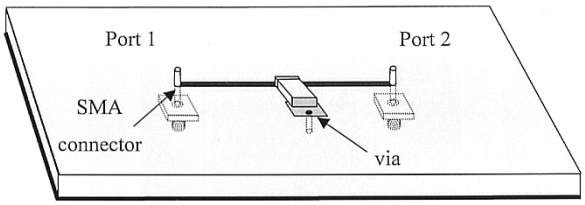

Fig. 3. Test board with a one-capacitor, low-pass filter.

III. Laboratory Measurements of Low-Pass Filters

Two types of low-pass filters were measured, a single-capacitor filter and a two-capacitor filter. The low-pass filters were mounted on test boards as shown in Fig. 3. A top view of

Manuscript received August 10, 2002; revised March 20, 2003.

T. M. Zeeff is with the Hewlett-Packard Company, San Diego, CA 92127 USA (e-mail: tzeeff@ece.umr.edu).

T. H. Hubing, T. P. Van Doren, and D. Pommerenkd are with the Department of Electrical and Computer Engineering, Electromagnetic Compatibility Laboratory, University of Missouri-Rolla, MO 65409 USA (e-mail: tzeeff@ece.umr.edu; hubing@umr.edu).

Digital Object Identifier 10.1109/TEMC.2003.819059

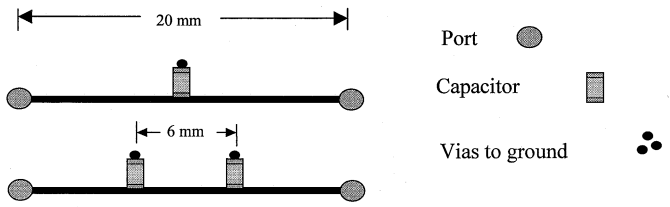

Fig. 4. Top-down view of two different filter configurations; one-capacitor filter, and a two-capacitor filter.

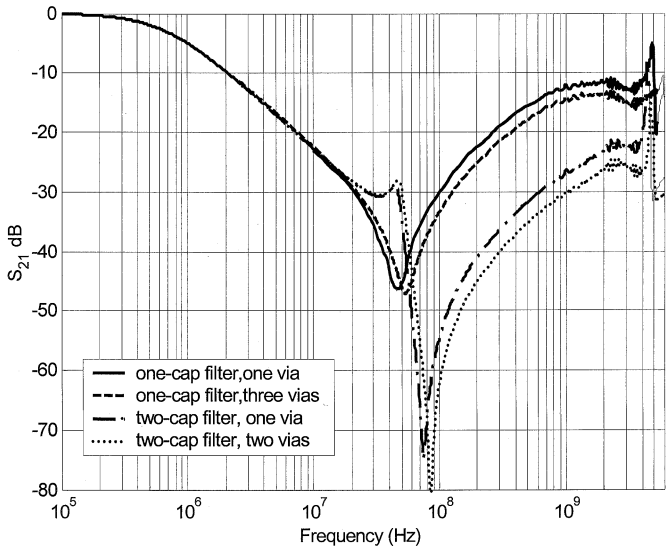

Fig. 5. Measured results of the filter configurations shown in Fig. 4.

the filter configurations is shown in Fig. 4. SMA connectors were placed on the test board and connected to both ends of a 20-mm-long microstrip trace. A filter consisting of a single 10-nF capacitor or two 4.7-nF capacitors spaced 6 mm apart was attached to the trace. The capacitors were connected to the signal return plane by one or two vias. The PCB dielectric was 1.1-mm (43 mil) thick. The magnitude of the voltage transfer coefficient $|S_{21}|$ was measured with a network analyzer. The measured results are shown in Fig. 5.

Below 20 MHz, all four filter configurations behave similarly and the connection inductance is not a significant factor. Above 50 MHz, the response of the one-capacitor filter is a function of the mutual inductance (due to flux wrapping the body of the capacitor and the vias). Employing two vias instead of one reduces the coupled signal by only a few decibels. This suggests that the majority of coupled flux wraps the body of the capacitor.

If the filter had been modeled as a simple *LC* circuit rather than an *MLC* circuit, the two-capacitor filter would have half the total inductance and therefore exhibit a 6-dB improvement at high frequencies. However, the measured results in Fig. 5 show that the two-capacitor filter outperforms the one-capacitor filter at high frequencies by approximately 10–15 dB.

IV. Analysis of Two-Capacitor Filter

To further characterize the performance of the two-capacitor filter, the effects of the capacitor spacing and the dielectric height were examined. The spacing between the capacitors of

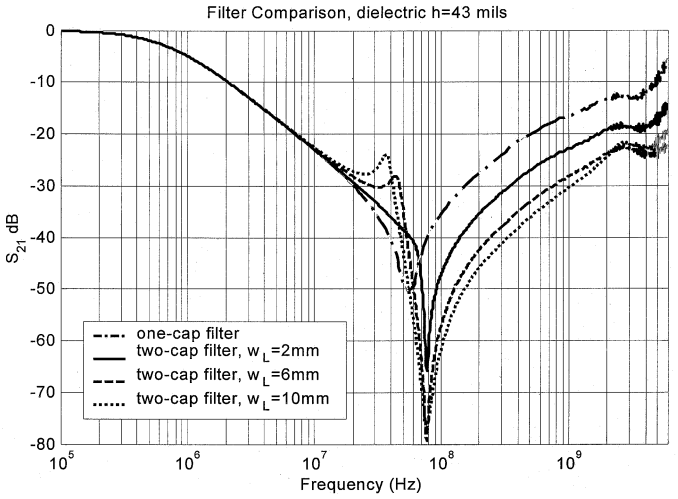

Fig. 6. Measured results of the two-capacitor filter when the via spacing was varied, $h = 1.1$ mm.

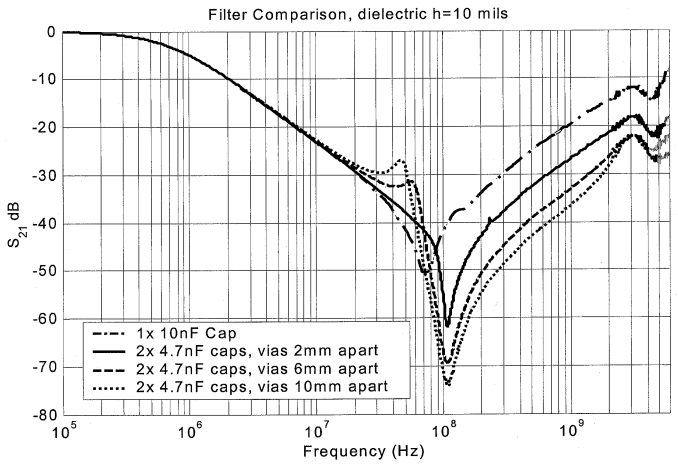

Fig. 7. Measured results of the two-capacitor filter when the via spacing was varied, $h = 0.25$ mm.

the two-capacitor filter was varied from 2 to 10 mm on the test board. The measured results are shown in Fig. 6. The signal trace on the test board was 20-mm long for all measurements. The dielectric was 1.1-mm thick for this test board. It is evident that the spacing between the capacitors can have a significant impact on the performance of the filter at high frequencies. When the via spacing is only 2 mm, the two-capacitor filter outperforms the one-capacitor filter by approximately 6 dB above a few hundred megahertz. When the via spacing is changed to 6 mm, the filter performance improves by another 5 dB. When the via spacing is increased to 10 mm, the filter performance improves by another 3 dB.

To reduce the loop area associated with flux wrapping the capacitor, another test board with a 0.25-mm (10-mil) thick dielectric was constructed. The filter configurations in Fig. 4 were re-evaluated with the new board. The measured results are shown in Fig. 7. The performance of the various filter types with a 0.25-mm dielectric is similar to the performance observed with a 1.1-mil dielectric. The only significant difference is that, for all filter types, the $|S_{21}|$ from 200 MHz to 2 GHz is lower

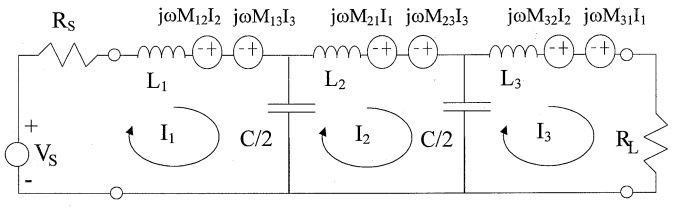

Fig. 8. Equivalent circuit for a two-capacitor filter.

with the thinner dielectric due to lower mutual inductance. Overall, the performance of the two-capacitor filter improved as the capacitor spacing was increased, and the high-frequency performance of the two-capacitor filter with a 10-mm spacing was nearly 17 dB better than that of the one-capacitor filter.

V. Lumped-Element Model of Two-Capacitor Filter

An equivalent circuit for the two-capacitor filter is shown in Fig. 8. Each loop of the filter has a self-inductance L_i and there is a mutual inductance between each of the loops, M_{ij}, shown as a current-dependent voltage source. The mutual inductance M_{ij} is the magnetic flux in loop i due to the current I_j in loop j divided by the current I_j. The frequency response of a two-capacitor filter is compared to the frequency response of a one-capacitor filter in Fig. 9.

From circuit analysis, it is apparent that the performance of the two-capacitor filter is related to the mutual inductance between the input and output loops just like it is with the one-capacitor filter. However, above the *MC* resonance frequency, the $|S_{21}|$ of the two-capacitor filter increases proportional to $(M_{12})^2/(L_2+M_{13})$ instead of *M*. At higher frequencies, with the two-capacitor configuration, the coupling between the input and output loops is rather small, approximately $(k_{13}+k_{12}k_{23})$. The improved performance of the two-capacitor filter can be attributed to two things. First, the middle loop physically separates the input and output loops such that the flux directly linking the input and output loops is reduced. Secondly, the addition of the middle loop means that the magnetic flux coupling the input and middle loop must again magnetically couple from the middle loop to the output loop to reach the load.

Fig. 10 compares the measured $|S_{21}|$ to the $|S_{21}|$ of the lumped-element model circuits. The values for the lumped element self-inductances L_i were obtained from a PCB trace impedance calculator. The values for the mutual inductance were derived from a curve fit with the measured results. The filter characteristics seem to be accurately represented by the lumped-element circuit below a few gigahertz. Note that the sharp resonance at about 50 MHz in the model response is significantly damped in the measurement. This resonance corresponds to the series *LC* resonance of the middle loop. Additional simulations showed that this resonance is easily damped by accounting for a small amount of equivalent series resistance in the two capacitors.

VI. Estimating Mutual Inductance

It would be useful to find a way to estimate the mutual inductance without making a measurement. One way to estimate

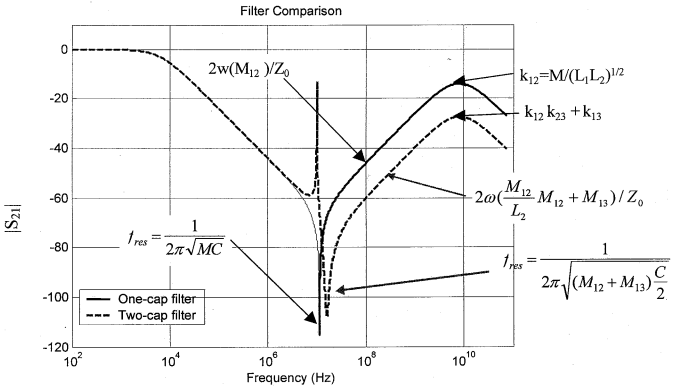

Fig. 9. Filter response of the two-capacitor and one-capacitor equivalent circuits.

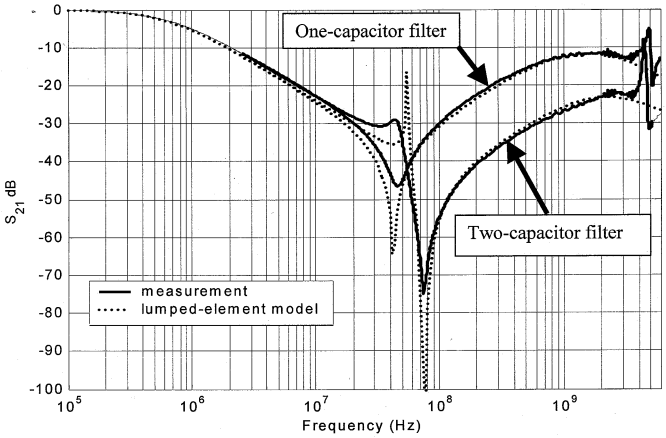

Fig. 10. Measurements of the filters compared to results obtained from the lumped-element circuit models.

the mutual inductance, M_{ij}, is to model the capacitor portion of the filter using rectangular wire loop segments. The effect of the magnetic flux wrapping the capacitor and coupling the input to the output can be expressed in terms of self- and mutual-partial inductances [3], [4]. An expression for partial (or branch) inductance (i.e. the self-partial inductance minus the mutual-partial inductance) of a filamentary wire segment in a rectangular loop is given as [3], [5]

$$L_p = \frac{\mu_0}{2\pi}\left[-s+\sqrt{h^2+s^2}-h\cdot\ln\left(\frac{h+\sqrt{h^2+s^2}}{s}\right) -h+h\cdot\ln\left(\frac{2h}{a}\right)\right] \quad (1)$$

where h is the height of the wire segment, a is the radius of the wire, and s is the distance to the other parallel wire segment in the loop. When the distance s is large relative to the height of the segment; then, the expression for the partial inductance simplifies to

$$L_p = \frac{\mu_0 h}{2\pi}\left[\ln\left(\frac{2h}{a}\right)-1\right]. \quad (2)$$

To validate the use of (1) in this application, a full-wave electromagnetic (EM) modeling tool, the Numerical Electromag-

TABLE I
VALUES OF *M* DERIVED FROM NEC SIMULATIONS AND FROM (1) FOR THE ONE-CAPACITOR FILTER CIRCUIT SHOWN IN FIG. 11, $h = 0.2$ m

M (nH)

h = 0.2 m, S = 1m, aa = 0.062 mm

	L_p	NEC	% Difference
a = 0.125 mm	279	252	-9.4%
a = 0.062 mm	307	281	-8.4%
a = 0.015 mm	363	337	-7.2%

TABLE II
VALUES OF *M* DERIVED FROM NEC SIMULATIONS AND FROM (1) FOR THE ONE-CAPACITOR FILTER CIRCUIT SHOWN IN FIG. 11, $h = 0.4$ m

M (nH)

h_l = 0.4 m, S = 1m, aa = 0.062 mm

	L_p	NEC	% Difference
a = 0.125 mm	605	555	-8.3%
a = 0.062 mm	661	611	-7.5%
a = 0.015 mm	775	723	-6.7%

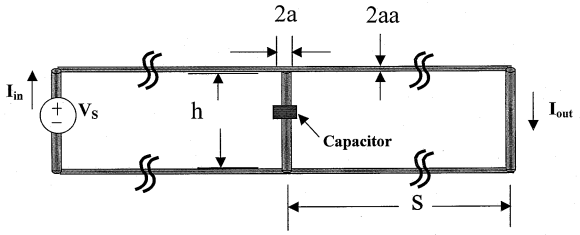

Fig. 11. One-capacitor filter circuit used in the NEC simulation.

netics Code (NEC) [6], was used to model simple capacitor filters. NEC is well suited for modeling and solving electromagnetic problems involving thin wires geometries. Several test circuits were modeled using NEC and the values of M_{ij} were extracted from the *MC* resonances of the simulation results. The values of M_{ij} from the simulations were compared to the partial inductances calculated using (1) and (2).

The results are shown in Tables I and II for the simple one-capacitor filter shown in Fig. 11. The model of the one-capacitor filter consists of a pair of rectangular loops that share one side. A capacitance was placed in the center segment. An ideal voltage source, placed near one end of the circuit, was used to drive the circuit. Y parameters were calculated from $I_{\rm in}$ and $I_{\rm out}$ shown in Fig. 11. The values of $I_{\rm in}$ and $I_{\rm out}$ were taken at the middle of the vertical wire segments at the ends of the circuit. S parameters were then derived from the Y parameters and the mutual inductance was calculated from the *MC* resonance of $|S_{21}|$. The difference between the partial inductance calculated with (1) and the mutual inductance calculated with the NEC software is around 10% for both of the circuits tested.

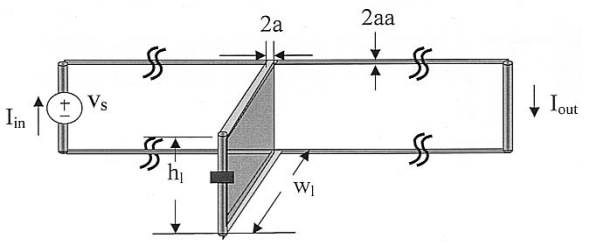

Fig. 12. One-capacitor filter with a side loop.

TABLE III
TEST RESULTS COMPARING *M* FROM NEC SIMULATIONS AND FROM (1) FOR ONE-CAPACITOR FILTER CIRCUIT SHOWN IN FIG. 12

M (nH)

h_l = 0.2 m, w_l = 0.1 m, aa = 0.062 mm

	L_p	NEC	% Difference
a = 0.125 mm	524	508	-2.9%
a = 0.062 mm	580	563	-3.0%
a = 0.015 mm	694	675	-2.7%

TABLE IV
TEST RESULTS COMPARING M FROM THE NEC SIMULATIONS AND FROM (1) FOR THE ONE-CAPACITOR FILTER CIRCUIT SHOWN IN FIG. 12

M (nH)

h_l = 0.2 m, w_l = 0.4 m, aa = 0.062 mm

	L_p	NEC	% Difference
a = 0.125 mm	1390	1416	+1.9%
a = 0.062 mm	1530	1556	+1.7%
a = 0.015 mm	1814	1838	+1.3%

For practical reasons, filter capacitors are not normally mounted directly below the trace on a printed circuit board, but are mounted out to the side of the trace. Fig. 12 shows a circuit where the capacitor is mounted on a loop that extends out from the trace. The mutual inductance is calculated as the sum of the branch inductances of all three segments of the capacitor loop [5]. This mutual inductance is compared to the mutual inductance calculated with the NEC software. The results are shown in Table s III and IV. For the two circuits modeled, the difference between the mutual inductance calculated with (1) and with the NEC software was around 3%.

Next, the two-capacitor filter configuration shown in Fig. 13 was modeled with the NEC software. The overall effective mutual inductance, $M_{12} + M_{13}$, was extracted from the simulation and compared to the partial inductance approximation of the mutual inductance, M_{12}, calculated using (1). The results are shown in Table V. The difference between the mutual inductance extracted from the NEC simulations and the mutual inductance calculated with (1) is about 10%.

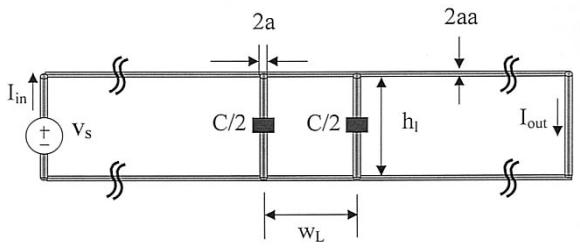

Fig. 13. Model of the two-capacitor filter.

TABLE V
TEST RESULTS COMPARING *M* FROM NEC SIMULATIONS AND FROM (1) FOR CIRCUIT SHOWN IN FIG. 13

Inductance (nH)

h_l = 0.2 m, w_L = 0.4 m, a = aa = 0.062 mm,

C = 10 nF, L_1=L_3=3600 nH, L_2=830 nH

	L_p	NEC
M_{12}	~300	--
$M_{12} + M_{13}$	--	~272

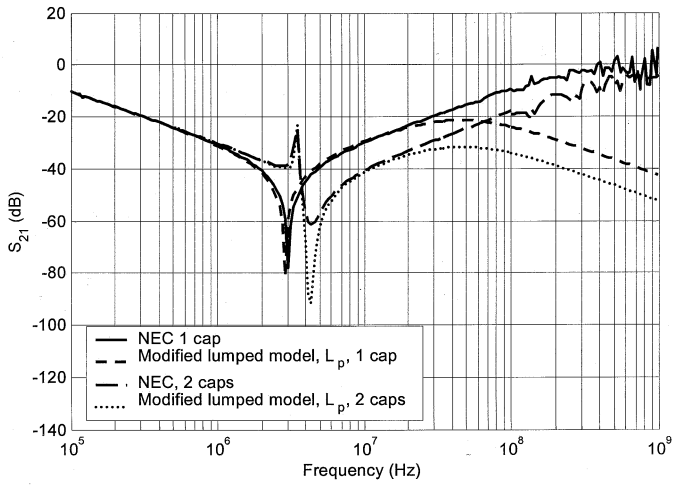

Fig. 14. Comparison between the filter response of the lumped element equivalent circuit and the NEC simulations.

VII. COMPARING EQUIVALENT CIRCUIT MODELS TO SIMULATION MODELS

Fig. 14 shows the filter responses obtained using NEC simulations and compares them to the results obtained from the equivalent circuit model. Values for M_{ij} in the circuit model were obtained from (1). The filter geometries used in Fig. 14 correspond to the filters in Fig. 11 and Fig. 13, where $h = 0.2$ m, $a = 0.062$ mm, and the total circuit length was 2 m.

For all filter types evaluated, there is good agreement between the equivalent circuit model using mutual inductances calculated with (1) and the filter response calculated with the NEC software at low frequencies. However, at higher frequencies, where the circuit becomes large relative to a wavelength,

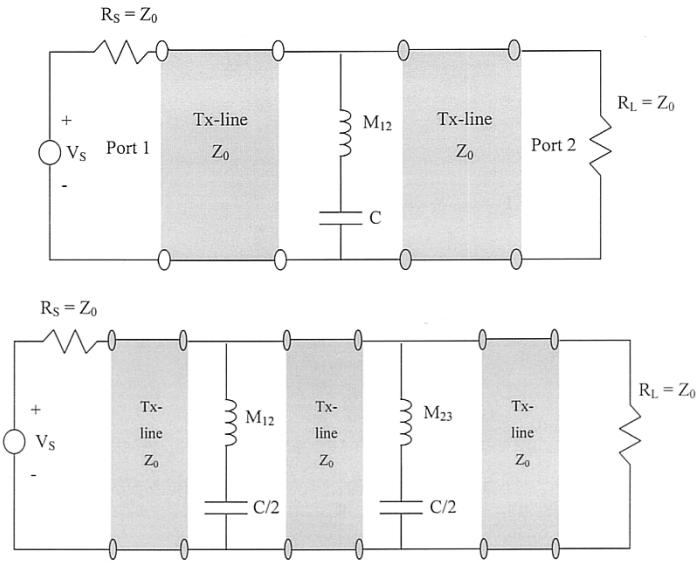

Fig. 15. Modified equivalent circuits of the one and two-capacitor filters.

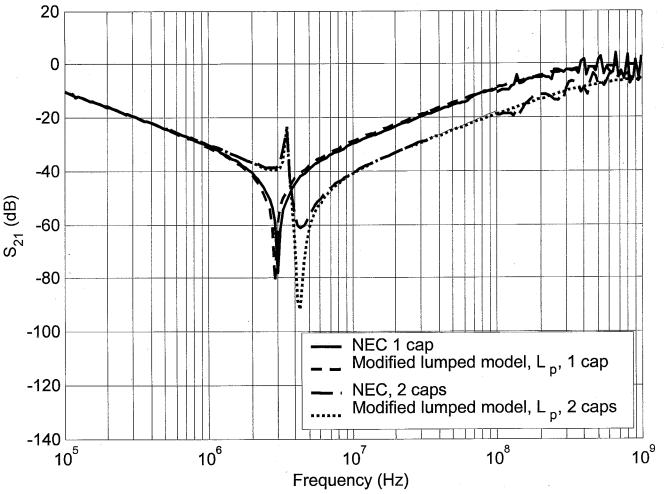

Fig. 16. Modified equivalent circuits of the one and two-capacitor filters compared with the NEC simulations.

the lumped element circuit does not predict transmission-line resonances. The filter response of the equivalent circuit levels off at high frequencies to k_{12} for the one-capacitor filter and to $k_{12}k_{23} + k_{13}$ for the two-capacitor filter. In the NEC simulations, the filter response does not level off, but rather continues to increase.

Instead of representing the input and output loops as lumped inductances, L_i, the model in Fig. 15 represents the input and output loops as transmission lines. The one-capacitor filter circuit consists of a series *MC* circuit, between the transmission-line segments. The two-capacitor filter is modeled similarly. Note that the two-capacitor filter model does not account for the mutual inductance between loop 1 and loop 3, M_{13}. For most filter geometries with significant spacing between the two capacitors, M_{13} is very small compared to M_{12} and M_{23}.

The filter responses from the modified circuit models and the NEC simulations are compared in Fig. 16. The filter responses

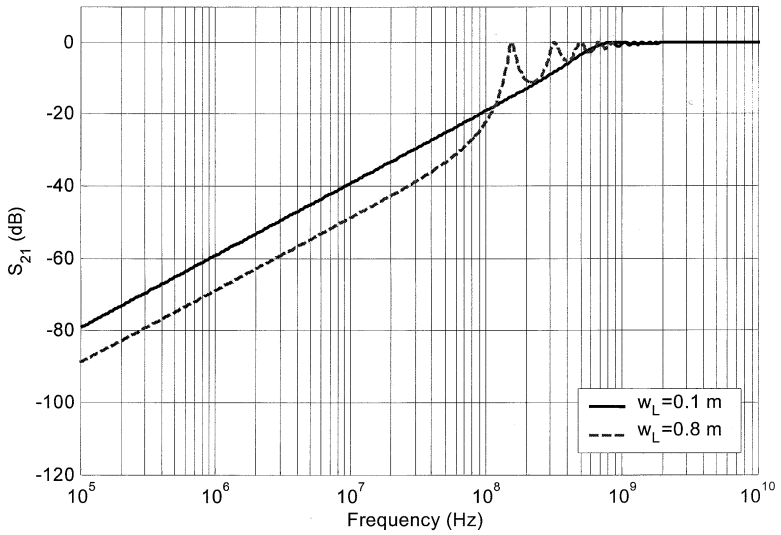

Fig. 17. Modified equivalent circuits of the two-capacitor filter for small w_L. Total circuit length is 20 m, $h = 0.2$ m, $a = \text{aa} = 0.062$ mm, $Z_0 = 1000\,\Omega$.

of the transmission-line circuit models now match the NEC simulations very well. Note that $|S_{21}|$ converges to 0 dB at high frequencies, not *M/L* or $k_{12}k_{23}+k_{13}$ as predicted by the equivalent circuits shown in Figs. 1 or 8.

VIII. Finding Optimum Spacing Between Capacitors of Two-Capacitor Filter

The results in the previous sections suggest that two-capacitor low-pass filters significantly outperform single-capacitor filters at frequencies above self-resonance. The high-frequency performance of the two-capacitor filter depends on the spacing between the capacitors. To determine the optimum spacing between the pair of capacitors in a two-capacitor filter, several test circuits with varying capacitor spacing were simulated using the NEC software. Based on the lumped element circuit for the two-capacitor filter, the optimum capacitor spacing would minimize the function $(M_{12})^2/(L_2 + M_{13})$. This would imply that the spacing should be as large as possible since M_{12} simplifies to (1), M_{13} goes to zero, and L_2 increases proportional to the loop width as the middle loop is widened.

Table VI shows the results obtained from (1) and from the NEC software for the effective mutual inductance $((M_{12})^2)/(L_2 + M_{13})$ as the distance between the capacitors, w_L, is increased. The data in Table VI supports the idea that the optimum spacing between the pair of capacitors in the two-capacitor filter, w_L, is as large as is possible, whether the mutual inductance is calculated with (1) or derived from the NEC simulations. From the data in Table VI, it is shown that doubling w_L will reduce S_{21} by 6 dB when $w_L > 5\ h$, whereas when $w_L < 5\ h$, doubling w_L will reduce S_{21} by less than 6 dB. This is because M_{12} does not increase significantly beyond $w_L > 5\ h$, whereas L_2 will continue to increase as w_L is increased.

However, at high frequencies, where the loops are not electrically small, the concept of a loop inductance, L_2, is no longer useful. The transmission-line equivalent circuit in Fig. 15(b)

TABLE VI
Effects of Increasing Spacing Between Pair of Capacitors, w_L, on High-Frequency Response of Two-Capacitor Filter

a = 0.062 cm, h = 0.20 m				$(M_{12})^2/L_2 + M_{13}$ (nH)	
w_L (m)	M_{12} (nH)	M_{13} (nH)	L_2 (nH)	Partial Inductance Equations, (1)	NEC Software
Total trace length = 2 m					
0.10	278.0	29.2	830	122	97
0.20	292.3	15.1	1170	88	65
0.40	301.2	6.5	1825	56	38
0.80	306.0	2.1	3120	32	20
1.60	308.5	0.3	5700	17	9.4
Total trace length = 20 m					
1.60	308.5	2.1	5700	19	6.8
3.20	309.7	0.9	10900	10	3.5
6.40	310.4	0.3	21200	4.9	1.8
12.80	310.7	0.07	41900	2.3	0.9

was used to show what happens to the filter response as the capacitor separation is increased beyond the point where it can be considered electrically small. Figs. 17 and 18 show $|S_{21}|$ for four of the circuit configurations used in Table VI. For all of these simulations, the capacitance was set to a high value (0.01 F) so that the *MC* resonance would occur below the lowest frequency shown in the plots.

As shown in Table VI, as the middle loop width, w_L, is increased, $|S_{21}|$ decreases in proportion to $((M_{12})^2)/(L_2+M_{13})$. However, as w_L approaches a half wavelength, a resonant peak occurs in $|S_{21}|$. After this resonance, $|S_{21}|$ fluctuates with an average value that increases rapidly until $|S_{21}|$ reaches 0 dB. As indicated in Fig. 18, wider middle loops will result in lower coupling above the *MC* resonance as long as the spacing is electrically small at the frequencies of interest. When choosing the separation between the pair of capacitors, this must be taken into consideration.

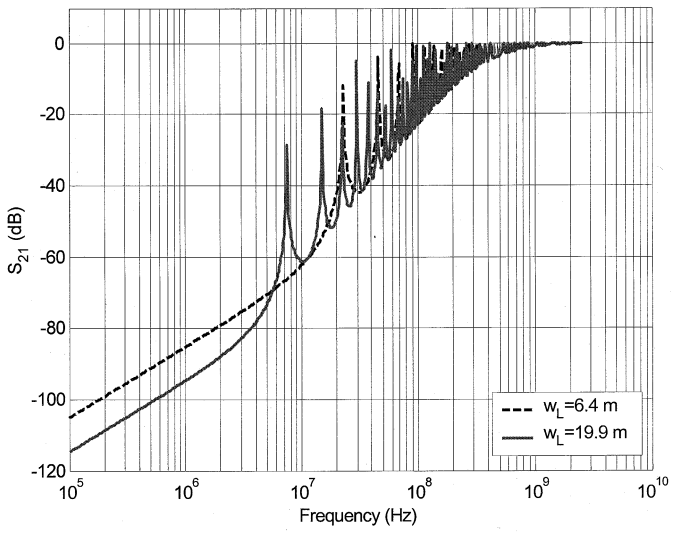

Fig. 18. Modified equivalent circuits of the two-capacitor filter for large w_L. Total circuit length is 20 m, $h = 0.2$ m, $a = \mathrm{aa} = 0.062$ mm, $Z_0 = 1000\ \Omega$.

IX. Conclusion

The performance of low-pass filters consisting of a single capacitor is limited by the magnetic coupling between the input and output sides of the filter. To improve the high-frequency performance of a low-pass filter, the mutual inductance between the input and output sides of the filter must be reduced.

A filter consisting of two appropriately spaced capacitors can be much more effective at high frequencies than a single-capacitor filter. The improved performance of the two-capacitor filter can be attributed to two things. First, the middle loop physically separates the input and output loops such that the magnetic flux directly linking the input and output loops is reduced. Second, the addition of the middle loop means that the magnetic flux coupling the input and middle loop must again magnetically couple from the middle loop to the output loop to reach the load. The lower effective mutual inductance between the input and output sides of the filter results in improved performance at high frequencies.

An estimate for the effective mutual inductance can be obtained using equations for the partial (or branch) inductance of the capacitor connection. In simulations of wire geometries, the mutual inductance calculated using the partial inductance formula was within 10% of the numerical simulation. The mutual inductance calculated with the partial inductance formula can then be used in an equivalent circuit to accurately model the filter.

The optimum configuration of the two-capacitor filter depends on the spacing between the pair of capacitors. As the spacing between the pair of capacitors increases, the filter response at high frequencies improves. However, when the length of the loop created by the pair of capacitors approaches a half wavelength long, the filter response degrades rapidly.

References

[1] C. N. Olsen, "Understanding and improving shunt capacitor high-frequency attenuation," M.S. thesis, Dep. Elect. Comp. Eng., Univ. Missouri-Rolla, Rolla, 2000.

[2] T. M. Zeeff, "Analysis of a prototype low-mutual inductance, low pass filter," Ph.D. dissertation, Dep. Elect. Comp. Eng., Univ. Missouri-Rolla, Rolla, 2002.

[3] A. E. Ruehli, "Inductance calculations in a complex integrated circuit environment," *IBM J. Res. Dev.*, vol. 16, no. 5, pp. 470–481, 1972.

[4] C. R. Paul, "Modeling electromagnetic interference properties of printed circuit boards," *IBM J. Res. Dev.*, vol. 33, no. 1, pp. 33–50, 1989.

[5] D. M. Hockanson, J. L. Drewniak, R. E. DuBroff, T. H. Hubing, and T. P. Van Doren, "Considerations for magnetic-field coupling resulting in radiated EMI," in *Proc. 1998 IEEE Int. Symp. Electromagnetic Compatibility*, Denver, CO, Aug. 1998, pp. 808–813.

[6] G. J. Burke and A. J. Poggio, "Numerical Electromagnetics Code (NEC)—Method of Moments," Naval Ocean Systems Center, San Diego, CA, NOSC Tech. Document 116, Jan. 1981.

Theodore M. Zeeff received the B.S., M.S., and Ph.D. degrees from the University of Missouri-Rolla, in 1997, 1998, and 2002, respectively.

He is currently an EMC Engineer for Hewlett-Packard Company, San Diego, CA.

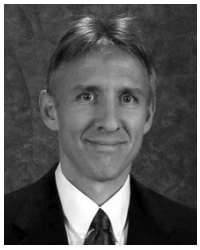

Todd H. Hubing (S'82–M'82–SM'93) received the B.S.E.E. degree from the Massachusetts Institute of Technology, Cambridge, in 1980, the M.S.E.E. degree from Purdue University, West Lafayette, IN, in 1982, and the Ph.D. degree in electrical engineering from North Carolina State University, Raleigh, in 1988.

He is currently a Professor of electrical engineering with the University of Missouri-Rolla (UMR), where he is also a member of the principal faculty in the Electromagnetic Compatibility Laboratory. Prior to joining UMR in 1989, he was an Electromagnetic Compatibility Engineer with IBM, Research Triangle Park, NC. Since joining UMR, the focus of his research has been measuring and modeling sources of electromagnetic interference. He has authored or presented over 100 technical papers, presentations, and reports on electromagnetic modeling and electromagnetic compatibility related subjects.

Dr. Hubing has been a member of the Board of Directors of the IEEE Electromagnetic Society since 1995 and is the 2002–2003 President of the Society.

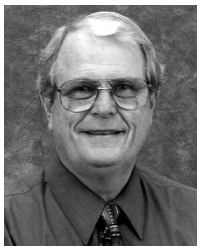

Thomas P. Van Doren (S'60–M'69–SM'96–F'02) received the B.S., M.S., and Ph.D. degrees from the University of Missouri-Rolla (UMR), in 1962, 1963, and 1969, respectively.

He is a Professor of Electrical and Computer Engineering at UMR. For the past 23 years, he has specialized in electromagnetic compatibility education and research. Over 17 000 engineers and technicians have attended his short course on "Grounding and Shielding of Electronic Systems."

David Pommerenke (M'98) was born on April 11, 1962 in Ann Arbor, MI. He received the diploma in electrical engineering, and the Ph.D. degree in "transient fields of electrostatic disturbance (ESD)," from the Technical University Berlin, Berlin, Germany, in 1989, and 1995, respectively.

He joined the Hewlett-Packard Company in 1996 and became an Associate Professor in the Electromagnetic Compatibility Group at the University of Missouri-Rolla, in 2001. His areas of interest are EMC, ESD, numerical calculation, high-voltage partial discharge detection systems, electronics and design of test and measurement equipment. As relevant to the ESD work, he is member of the International Electrotechnical Commission (IEC), Geneva, Switzerland, IEC TC77b WG-9, the working group that sets the IEC 61 000-4-2 ESD test standard.